Structural Engineering and Mechanics, Vol. 3, No. 3 (1995) 229-244
DOI: http://dx.doi.org/10.12989/sem.1995.3.3.229

Effects of damping on the parametric instability behaviour of plates under localized edge loading (compression or tension)

P.J. Deolasi† and P.K. Datta‡

Department of Aerospace Engineering, Indian Institute of Technology, Kharagpur 721302, India

Abstract. The parametric instability behaviour of a plate subjected to localized in-plane compressive or tensile periodic edge loading is studied, considering the effects of damping into the system. Different edge loading cases have been considered. Damping has been introduced in the form of proportional damping. Dynamic instability behaviour under compressive or tensile periodic edge loading shows that the instability regions are influenced by the load band width and its location on the edge. The effects of damping on the instability regions show that there is a critical value of dynamic load factor beyond which the plate becomes dynamically unstable. The critical dynamic load factor increases as damping increases. Damping generally reduces the widths of the instability regions.

Key words: plate; edge loading; compression; tension; damping; parametric instability.

1. Introduction

The vibration and buckling behaviour of plates involving uniform pre-buckle stress states have been extensively studied and results well documented (Timoshenko and Gere 1961, Leissa 1969). There are, however, many practical plate stability problems in which the pre-buckle stress states are non-uniform. The situation in which loads are applied over only parts of the edges causing non-uniform initial stresses has been studied (Rockey and Bagchi 1970, Khan and Walker 1972, Spencer and Surjanhata 1985) for static stability behaviour. The free vibration analysis of rectangular plate subjected to a pair of oppositely directed in-plane concentrated forces has been studied by Leissa and Ayoub (1988).

Plates can also buckle when subjected to forces that are only tensile. Such buckling can occur whenever solution to the plane elasticity problem yields internal stresses that are compressive in any direction at any point. Tension buckling of rectangular sheets due to concentrated forces has recently been studied by Leissa and Ayoub (1989).

Structural elements subjected to in-plane periodic forces may induce transverse vibrations, which may be resonant for certain combinations of natural frequency of transverse vibration, the frequency of the in-plane forcing function and the magnitude of the in-plane load. The spectrum of values of parameters causing unstable motion is referred to as the region of dynamic instability or parametric resonance. Bolotin, in his text on dynamic stability (1964), gives a thorough review of the problems involving parametric excitation of structural elements. Hutt and

† Research Scholar
‡ Professor

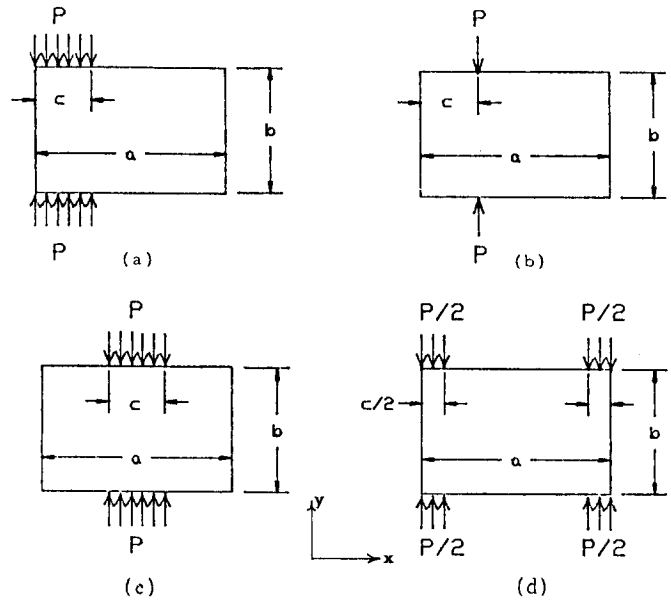

Fig. 1 Description of the plate problems
(a) Partial edge loading at one end, (b) Concentrated edge loading,
(c) Partial edge loading at the centre, (d) Loading at both ends.

Salam (1971) used a thin plate finite element model to study the dynamic instability of plates subjected to uniform periodic edge loading.

The influence of damping on the dynamic behaviour of plates become more pronounced with the use of special damping treatment to enhance the damping properties of the structure for vibration control. The effect of damping on vibration behaviour of plates by the use of viscoelastic layer is found in the literature (Ioannides and Grootenhuis 1979).

The effect of damping on the dynamic instability behaviour of beams has been studied (Bolotin 1964, Engel 1991). Parametric excitation behaviour of plates with damping subjected to uniform in-plane loading has also been studied (Hutt and Salam 1971, Cederbaum 1992). However, there is no work available in the literature on the dynamic instability behaviour of plate with damping subjected to non-uniform in-plane loading.

The present paper deals with the study of effects of damping on dynamic instability behaviour of plates subjected to localized edge loading, either compressive or tensile. The concept of proportional damping has been used in the present analysis. Finite element formulation is applied for obtaining initial non-uniform stress distribution in the plate and to solve the buckling, vibration and dynamic stability problems.

2. Analysis

The problem considered here consists of a rectangular plate ($a \times b$) subjected to in-plane localized edge loading as shown in Fig. 1. The loading shown is compressive in nature. Reversing the direction of loading will give the corresponding tensile loading problems. The boundaries of the plate are simply supported along all the edges.

Eight noded quadratic isoparametric element is used in the present analysis. Three displacement

components w, θ_x and θ_y are specified at each node. Mindlin's hypothesis is applied to include the effects of transverse shear deformation and rotary inertia.

The expressions for the total potential energy and the kinetic energy of the plate are as follows.

Total potential energy:

$$U=\int_0^a\int_0^b\left\{\frac{D}{2}\left[\left(\frac{\partial\theta_y}{\partial x}\right)^2+\left(\frac{\partial\theta_x}{\partial y}\right)^2-2\nu\left(\frac{\partial\theta_y}{\partial x}\right)\left(\frac{\partial\theta_x}{\partial y}\right)+(1-\nu)\left(\frac{\partial\theta_x}{\partial x}-\frac{\partial\theta_y}{\partial y}\right)^2\right]\right.$$
$$+\frac{kEh}{2(1+\nu)}\left[\left(\frac{\partial w}{\partial x}-\theta_y\right)^2+\left(\frac{\partial w}{\partial y}+\theta_x\right)^2\right]\Big\}dydx+\int_0^a\int_0^b\left\{\frac{h}{2}\left[\sigma_x\left(\frac{\partial w}{\partial x}\right)^2+\sigma_y\left(\frac{\partial w}{\partial y}\right)^2\right.\right.$$
$$\left.+2\tau_{xy}\left(\frac{\partial w}{\partial x}\frac{\partial w}{\partial y}\right)\right]+\frac{h^3}{24}\left[\sigma_x\left\{\left(\frac{\partial\theta_x}{\partial x}\right)^2+\left(\frac{\partial\theta_y}{\partial x}\right)^2\right\}+\sigma_y\left\{\left(\frac{\partial\theta_x}{\partial y}\right)^2+\left(\frac{\partial\theta_y}{\partial y}\right)^2\right\}\right.$$
$$\left.\left.+2\tau_{xy}\left\{\frac{\partial\theta_x}{\partial x}\frac{\partial\theta_x}{\partial y}+\frac{\partial\theta_y}{\partial x}\frac{\partial\theta_y}{\partial y}\right\}\right]\right\}dydx \tag{1}$$

and kinetic energy:

$$T=\rho\int_0^a\int_0^b\left[\frac{h}{2}\left(\frac{\partial w}{\partial t}\right)^2+\frac{h^3}{24}\left\{\left(\frac{\partial\theta_x}{\partial t}\right)^2+\left(\frac{\partial\theta_y}{\partial t}\right)^2\right\}\right]dydx \tag{2}$$

where D is the plate flexural rigidity and $D=Eh^3/12(1-\nu^2)$; σ_x, σ_y and τ_{xy} are the initial, in-plane stresses; k is the shear correction factor which accounts for the fact that transverse shear strain is not constant over the plate thickness. ($k=5/6$ is taken in the present analysis).

Upon assuming suitable interpolation functions for w, θ_x and θ_y in Eqs. (1) and (2) in terms of nodal displacements, the total potential energy and kinetic energy can be written in matrix form as

$$U=\frac{1}{2}\{q\}^T[K]\{q\}$$

$$T=\frac{1}{2}\{\dot{q}\}^T[M]\{\dot{q}\}$$

Damping is usually introduced in the dynamic analysis in terms of the energy dissipation in the system (Meirovitch 1967), which may be expressed as

$$F=\frac{1}{2}\{\dot{q}\}^T[C]\{\dot{q}\}$$

where $\{q\}$ is the vector of generalized co-ordinates, $[K]$ is the stiffness matrix, $[M]$ is the mass matrix and $[C]$ is the damping matrix.

The stiffness matrix can be split into two parts,

$$[K]=[K_e]-P[S]$$

where $[K_e]$ is the elastic stiffness matrix, $[S]$ is the stress stiffness matrix, also called the geometric stiffness matrix which is obtained from the in-plane stress distribution σ_x, σ_y and τ_{xy} and P is the magnitude of the edge load.

The damping matrix is taken to be the linear combination of mass matrix and elastic stiffness matrix (*i.e.*, damping is assumed to be proportional).

Applying the principle of virtual work, following equilibrium equation for the damped plate is obtained:

$$[M]\{\ddot{q}\}+[C]\{\dot{q}\}+[K]\{q\}=0 \tag{3}$$

Static buckling load is obtained by solving the following eigenvalue problem:

$$[K]\{q\}=0$$

or

$$[K_e]\{q\}-P_{cr}[S]\{q\}=0 \tag{4}$$

where P_{cr} is the static buckling load.

Assuming the solution in the form

$$\{q\}=\{q_0\}e^{st},$$

Eq. (3) changes to the following quadratic eigenvalue problem

$$s^2[M]\{q_0\}+s[C]\{q_0\}+[K]\{q_0\}=0 \tag{5}$$

Eq. (5) represents a system of n coupled differential equations. In case of proportional or classical damping, Eq. (5) can be decoupled into n individual equations by using the real modes of undamped vibration (Caughey and O'Kelly 1965). The solution to each equation can be obtained separately.

In case of general non-classical damping, the method due to Foss (1958) can be used to obtain solution to the free vibration problem of damped system represented by Eq. (5). The Eq. (5) can be rearranged as

$$\left\{s\begin{bmatrix}[0] & [M]\\ [M] & [C]\end{bmatrix}+\begin{bmatrix}-[M] & [0]\\ [0] & [K]\end{bmatrix}\right\}\begin{Bmatrix}sq_0\\ q_0\end{Bmatrix}=0 \tag{6}$$

Eq. (6) can be solved by generalized Jacobi rotation method for complex eigenvalues s. The eigenvectors automatically converge to the form $\{sq_0^T, q_0^T\}^T$. Recently Chen (1993) has proposed a co-ordinate transformation method for the eigensolution of damped structural system of the form Eq. (6) which reduces the size of the equation but which is of the same form as proposed by Foss.

2.1. Dynamic stability problem

For the problems described in Fig. 1, the edge load P is periodic and can be expressed in the form

$$P(t)=P_s+P_t\cos\Omega t \tag{7}$$

where P_s is the static load, P_t is the amplitude of pulsating load and Ω is the angular frequency of pulsating load. The stress distribution in the plate will be non-uniform and periodic and any element will be subjected to in-plane stresses of the form

$$\begin{aligned}\sigma_x&=\sigma_{xs}+\sigma_{xt}\cos\Omega t=\bar{a}P_s+\bar{b}P_t\cos\Omega t\\ \sigma_y&=\sigma_{ys}+\sigma_{yt}\cos\Omega t=\bar{c}P_s+\bar{d}P_t\cos\Omega t\\ \tau_{xy}&=\tau_{xys}+\tau_{xyt}\cos\Omega t=\bar{e}P_s+\bar{f}P_t\cos\Omega t\end{aligned} \tag{8}$$

In Eq. (8), $\sigma_{xs}=\bar{a}P_s$, $\sigma_{ys}=\bar{c}P_s$ and $\tau_{xys}=\bar{e}P_s$ are the static portions of σ_x, σ_y and τ_{xy} respectively, whereas the other terms are time dependent. $\bar{a}$, $\bar{b}$, $\bar{c}$, $\bar{d}$, $\bar{e}$ and $\bar{f}$ are constant multipliers.

Let $$P_s=\alpha P_{cr} \text{ and } P_t=\beta P_{cr} \tag{9}$$

where, α and β are the percentages of the static buckling load P_{cr} and are termed as static and dynamic load factors respectively. P_{cr} is obtained from the solution of Eq. (4).

Usually, P_{cr} is taken as the reference load. In the present analysis, for compressive loading, the buckling load for uniformly loaded plate is taken as the reference load. Whereas for tensile loading, the tensile buckling load corresponding to concentrated loading at one end of the edges, is taken as the reference load. Substituting Eq. (8) and (9) in Eq. (3), the following equation in matrix form is obtained.

$$[M]\{\ddot{q}\}+[C]\{\dot{q}\}+[[K_e]-\alpha P_{cr}[S_s]-\beta P_{cr}[S_t]\ \cos\Omega t]\ \{q\}=0 \tag{10}$$

In Eq. (10), the matrices $[S_s]$ and $[S_y]$ are given by

$$[S_s]=\bar{a}[S_x]+\bar{c}[S_y]+\bar{e}[S_{xy}]$$
$$[S_t]=\bar{b}[S_x]+\bar{d}[S_y]+\bar{f}[S_{xy}]$$

in which $[S_x]$, $[S_y]$ and $[S_{xy}]$ are the stability matrices associated with σ_x, σ_y and τ_{xy} respectively, for an element.

Eq. (10) represents a system of second order differential equations with periodic coefficients. The boundaries of the dynamic instability regions are formed by the periodic solutions of period T and $2T$, where $T=2\Pi/\Omega$. The boundaries of the primary instability regions (with period $2T$) are determined (Bolotin 1964) from the equation

$$\begin{bmatrix} [K_e]-\alpha P_{cr}[S_s]+\frac{\beta}{2}P_{cr}[S_t]-\frac{\Omega^2}{4}[M] & -\Omega[C] \\ \Omega[C] & [K_e]-\alpha P_{cr}[S_s]-\frac{\beta}{2}P_{cr}[S_t]-\frac{\Omega^2}{4}[M] \end{bmatrix}\begin{Bmatrix} q_1 \\ q_2 \end{Bmatrix}=0 \tag{11}$$

Eq. (11) can be rearranged as

$$\left\{\left(\frac{\Omega}{2}\right)^2\begin{bmatrix} -[M] & [0] \\ [0] & [M] \end{bmatrix}+\left(\frac{\Omega}{2}\right)\begin{bmatrix} [0] & -2[C] \\ -2[C] & [0] \end{bmatrix}\right.$$
$$\left.+\begin{bmatrix} [K_e]-\alpha P_{cr}[S_s]+\frac{\beta}{2}P_{cr}[S_t] & [0] \\ [0] & -([K_e]-\alpha P_{cr}[S_s]-\frac{\beta}{2}P_{cr}[S_t]) \end{bmatrix}\right\}\begin{Bmatrix} q_1 \\ q_2 \end{Bmatrix}=0 \tag{12}$$

The size of the dynamic stability problem in Eq. (12) is double that of the original free vibration problem. To reduce the computational effort, the size of the Eq. (12) is reduced by means of co-ordinate transformation as follows:

Consider the two free vibration problems:

$$\left[[K_e]-\alpha P_{cr}[S_s]+\frac{\beta}{2}P_{cr}[S_t]=\omega_1^2[M]\right]\{q_1\} \tag{13a}$$

$$\left[[K_e]-\alpha P_{cr}[S_s]-\frac{\beta}{2}P_{cr}[S_t]=\omega_2^2[M]\right]\{q_2\} \tag{13b}$$

Let $[\Lambda_1]$ and $[\Lambda_2]$ be the diagonal matrices containing first m eigenvalues of the problems (13a) and (13b) respectively in the diagonal elements. Let $[\phi_1]$ and $[\phi_2]$ be the corresponding

$n \times m$ modal matrices.

Let

$$\begin{Bmatrix} q_1 \\ q_2 \end{Bmatrix} = \begin{bmatrix} [\phi_1] & [0] \\ [0] & [\phi_2] \end{bmatrix} \begin{Bmatrix} \xi_1 \\ \xi_2 \end{Bmatrix}$$

Substituting in Eq. (12) and premultiplying by

$$\begin{bmatrix} [\phi_1]^T & [0] \\ [0] & [\phi_2]^T \end{bmatrix}$$

$$\left\{ \left(\frac{\Omega}{2}\right)^2 \begin{bmatrix} -[I] & [0] \\ [0] & [I] \end{bmatrix} + \left(\frac{\Omega}{2}\right) \begin{bmatrix} [0] & -2[\hat{C}] \\ -2[\hat{C}]^T & [0] \end{bmatrix} + \begin{bmatrix} [\Lambda_1] & [0] \\ [0] & -[\Lambda_2] \end{bmatrix} \right\} \begin{Bmatrix} \xi_0 \\ \xi_2 \end{Bmatrix} = 0$$

where

$$[\hat{C}] = [\phi_1]^T [C] [\phi_2]$$

or

$$\Omega^2 [\bar{M}] \{\xi\} + \Omega [\bar{C}] \{\xi\} + [\bar{K}] \{\xi\} = 0 \tag{14}$$

where

$$[\bar{M}] = \begin{bmatrix} -[I] & [0] \\ [0] & [I] \end{bmatrix}, \quad [\bar{C}] = 4 \begin{bmatrix} [0] & -[\hat{C}] \\ -[\hat{C}] & [0] \end{bmatrix} \text{ and } [\bar{K}] = 4 \begin{bmatrix} [\Lambda_1] & [0] \\ [0] & -[\Lambda_2] \end{bmatrix}$$

Eq. (14) is similar to Eq. (5) in form, and the method suggested by Foss (1958) for the solution of free vibration problem (5) can be used to solve Eq. (14). Real solutions for Ω correspond to the boundaries of parametric instability regions. The complex solution for Ω means that steady state oscillation can not be maintained for any value of the excitation frequency, for that particular mode.

2.2. Finite element formulation

Eight noded quadratic isoparametric element is used in the present analysis. Three displacement components w, θ_x and θ_y are specified at each node. The details of the formulation of the element matrices is given in Appendix.

The overall matrices $[K_c]$, $[S]$ and $[M]$ in Eq. (3) are obtained by assemblies of corresponding element matrices and after elimination of the rows and columns corresponding to zero displacements. The vector of generalized co-ordinates consists of only active nodal displacements.

In the present analysis, damping matrix is assumed in the following form:

$$[C] = \mu_k [K_c] + \mu_m [M] \tag{15}$$

The constants μ_k and μ_m are determined so as to give the desired damping ratios in the first two modes of vibration of an unloaded plate ($P=0$). μ_k and μ_m are given by

$$\mu_k = \frac{2(\omega_2 \zeta_2 - \omega_1 \zeta_1)}{(\omega_2^2 - \omega_1^2)}$$

$$\mu_m = \frac{2\omega_1 \omega_2 (\omega_2 \zeta_1 - \omega_1 \zeta_2)}{(\omega_2^2 - \omega_1^2)}$$

where ω_1 and ω_2 are the first two undamped natural frequencies, and ζ_1 and ζ_2 are the corresponding damping ratios.

The damping in the form given by Eq. (15) gives proportional damping for an unloaded

plate, but not when the plate is loaded by certain in-plane edge load. Nevertheless, it remains classical if the mode shapes of buckling given by Eq. (4) are same as those of undamped free vibration. This is true for a simply supported plate loaded uniaxially or biaxially uniformly over the edges. But under the localized edge loading, the original damping matrix, $[C]$ becomes weakly nonclassical.

Taking the advantages of symmetries of the stiffness, inertia and damping properties of the plate, only upper half of the plate is considered for loading cases shown in Figs. 1(a) and 1(b). For loading cases shown in Fig. 1(c) and 1(d) only upper left quarter of the plate is considered. This greatly reduces the computational efforts and memory space requirements.

2.3. Computation

A computer programme has been written to perform all the necessary computations. The plate is divided into a two dimensional array of rectangular elements. Element elastic stiffness matrices are obtained with 2×2 Gauss sampling points to avoid possible shear locking. This type of modeling sometimes may lead to singular or nearly singular stiffness matrix. But such problems have not been encountered in the present investigation. Element mass matrices are also obtained with 2×2 sampling points.

The geometric stiffness matrices associated with static and pulsating loadings, $[S_s]$ and $[S_t]$ respectively, are essentially the functions of the in-plane stress distributions in the element due to applied static and pulsating edge loadings. Since the stress field is non-uniform, plane stress analysis is carried out using finite element technique to determine the stresses at Gauss sampling points. Element geometric stiffness matrices are obtained with 3×3 Gauss sampling points.

Element matrices are assembled into global matrices, using skyline technique. Subspace iteration method is adopted throughout to solve the eigenvalue problems (4), (13a) and (13b). First six modal vectors from problems (13a) and (13b) each are used for modal transformation for Eq. (12) and finally to arrive at Eq. (14). Eq. (14) is then transformed into the form similar to that of Eq. (6) and generalized Jacobi rotation method is adopted to solve it.

The non-dimensional loads γ and non-dimensional frequencies λ are defined as:

$$\text{Non-dimensional loads, } \gamma = \frac{Pa}{D}$$

$$\text{Non-dimensional frequencies, } \lambda = \omega b^2 \sqrt{\rho h / D}$$

To check the validity of the programme, the buckling and undamped free vibration results are compared with those available in the literature. The comparisons are shown in Tables 1 and 2. All the results are obtained with 10×10 mesh for full plate.

Table 1 Comparison of non-dimensional buckling loads γ_{cr} for a plate subjected to concentrated compressive loading at the centre of two opposite edges

a/b	Present	Leissa and Ayoub (1988)
1.0	25.720	25.814
2.0	29.852	30.061
0.5	28.851	26.523

Table 2 Comparison of non-dimensional frequencies λ without in-plane load. (Figures within the brackets indicate the results of Leissa and Ayoub (1988))

a/b	λ			
	Mode 11	Mode 12	Mode 21	Mode 22
1.0	19.729 (19.739)	49.148 (49.348)	49.148 (49.348)	78.432 (78.957)
	Mode 11	Mode 21	Mode 31	Mode 12
2.0	12.282 (12.337)	19.582 (19.739)	31.362 (32.076)	39.398 (41.946)

3. Results and discussions

Dynamic instability results have been obtained for the four loading cases shown in Fig. 1. The four loading cases along with the load parameter c/a give different combinations of position of load and load band width along the edge.

3.1. Dynamic instability behaviour under compressive loading

Figs. 2 to 5 show the boundaries of first two dynamic instability regions of a square plate for different loading cases shown in Fig. 1 for $\alpha=0.2$ and β varying from 0 to 2. In each case, the plots are obtained for two different values of c/a without damping ($\zeta=0$) and with damping ($\zeta=0.05$ for each mode). Various effects on the dynamic instability regions are discussed below.

3.1.1. Effect of load band width and its position on the edge

For the position of load near the ends of the edges and loading of small band width, the widths of the dynamic instability regions are usually smaller. This can be seen from Fig. 2 and 5 for $c/a=0.2$ and Fig. 3 for $c/a=0.1$. On the other hand, if the loading of small band width is applied near the centre of the edges, the widths of the instability regions are usually larger than those in the former case as seen from Fig. 3 for $c/a=0.5$ and Fig. 4 for $c/a=0.2$. For nearly uniform edge loading (load band width slightly less than or equal to the length of the edge) the widths of the instability regions are moderate as seen from Fig. 2, 4 and 5 for $c/a=0.8$. This is because of the fact that for position of loading near the ends of the edges, the restraints of the supported edges have a stabilizing effect on the dynamic instability behaviour. For loading near the centre of the edges, the edge restraints are not much effective. For nearly uniform loading, the edge restraints have a moderate effect.

3.1.2. Effect of static load factor

It has been observed that as the static load factor α increases, the instability regions shift inwards on the frequency ratio axis and their widths increase.

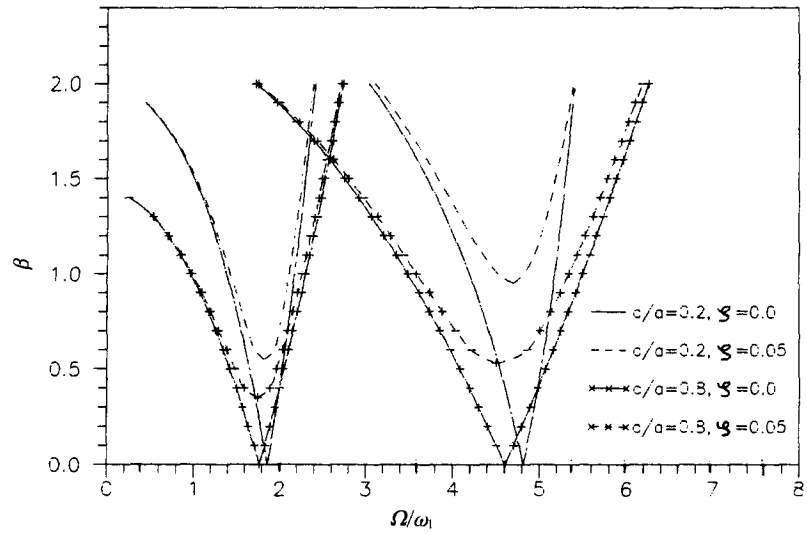

Fig. 2 Regions of dynamic instability for partial compressive edge loading at one end (α=0.2. a/b=1).

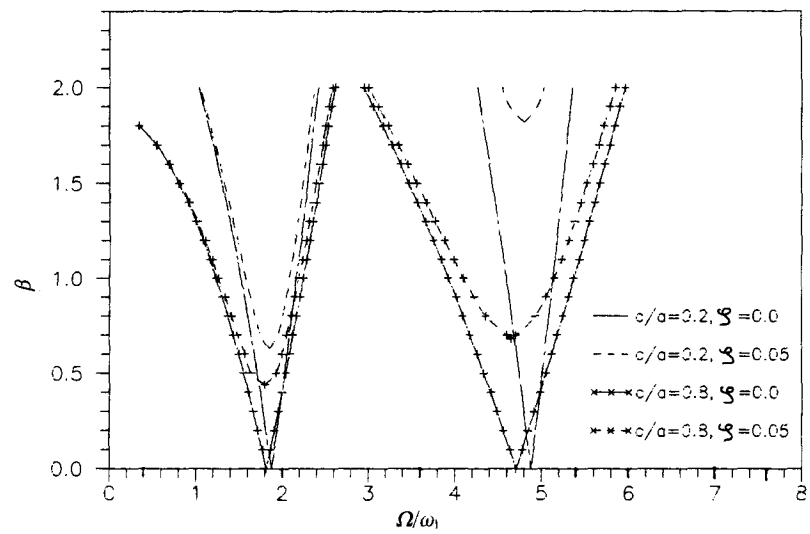

Fig. 3 Regions of dynamic instability for concentrated compressive edge loading (α=0.2. a/b=1).

3.1.3. Effect of damping

Effect of damping on the instability regions can clearly be seen in the Fig. 2 to 5. It can be observed that due to the presence of damping, the amplitude of the pulsating load must have a finite minimum value before the plate becomes dynamically unstable. The minimum value at which it occurs is termed as critical dynamic load factor. As the damping ratio increases, the critical dynamic load factor increases. It can also be seen that the presence of damping reduces the widths of instability regions. This indicates that the damping has stabilizing effects on the parametric instability behaviour.

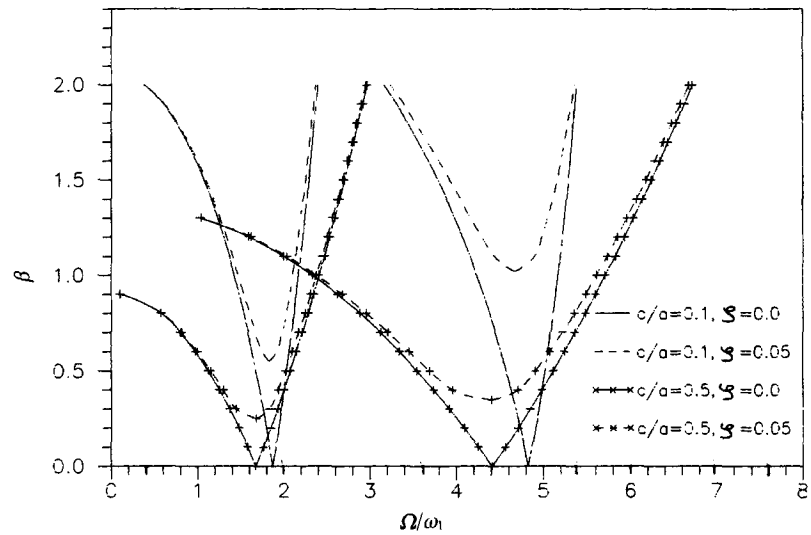

Fig. 4 Regions of dynamic instability for partial compressive edge loading at the centre ($\alpha=0.2$. $a/b=1$).

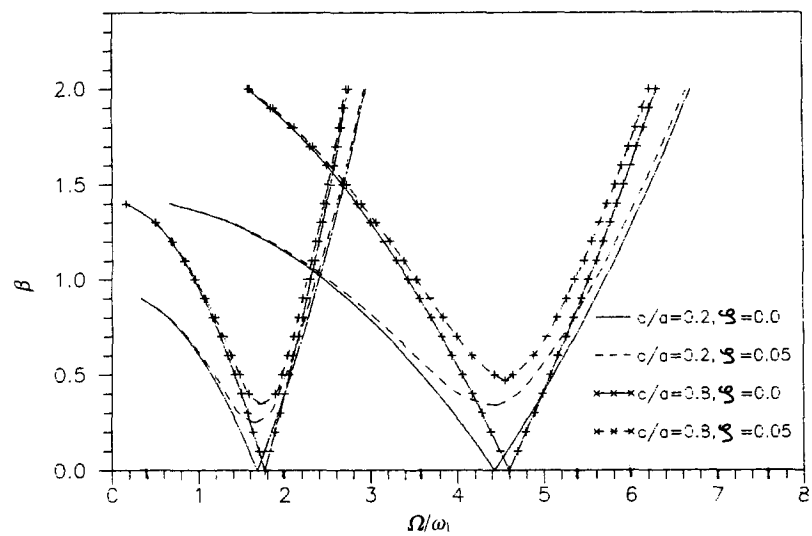

Fig. 5 Regions of dynamic instability for partial compressive edge loading at both ends ($\alpha=0.2$. $a/b=1$).

The influence of damping on the dynamic instability behaviour of plates for different edge loading cases has been studied. The damping has pronounced effects on the dynamic instability behaviour of plates subjected to localized edge loading near the ends of the edges as can be seen from the Fig. 2, 3 and 5. For partial edge loading at one or at both ends, as the width of the edge loading increases, the critical dynamic load factor decreases (Fig. 2 and 5), indicating more susceptibility to instability. For concentrated edge loading, as the load moves from the end of the edge to the centre, the critical dynamic load factor decreases as can be seen from Fig. 3.

Damping has less pronounced effects for loading of small band width near the centre of the edges. As the load band width increases, the critical dynamic load factor increases (Fig. 4), indicating less susceptibility to instability.

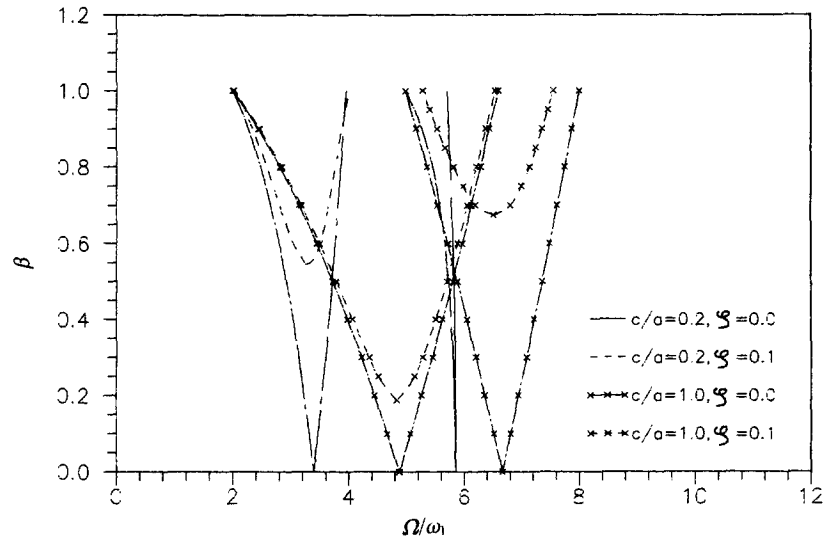

Fig. 6 Regions of dynamic instability for partial tensile edge loading at one end (α=0.5. a/b=1).

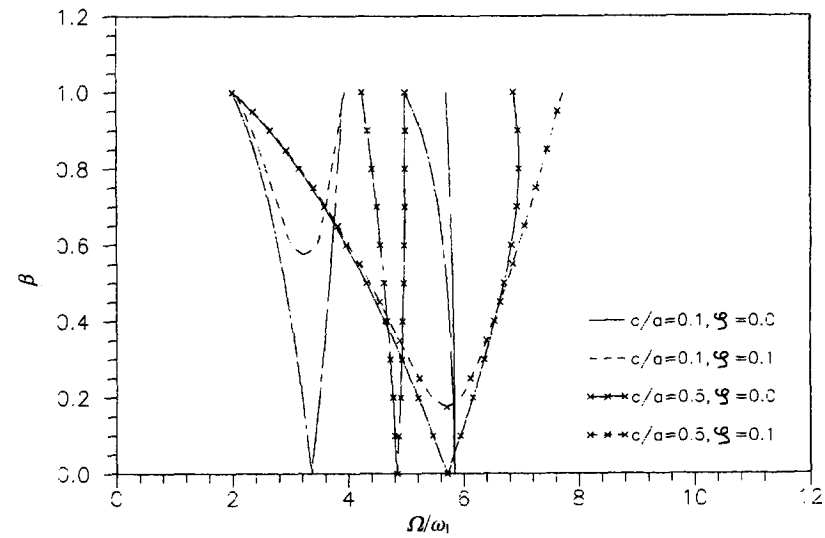

Fig. 7 Regions of dynamic instability for concentrated tensile edge loading (α=0.5. a/b=1).

3.2. Dynamic instability behaviour under tensile loading

The localized tensile edge loading acting on the plate producing compressive stresses within the plate will also cause dynamic instability of the plate. Figs. 6 to 9 show the boundaries of first two dynamic instability regions of a square plate for the same loading cases as in the case of compressive loading for α=0.5 and β varying from 0 to 1 without damping (ζ=0) and with damping (ζ=0.1). It can be observed that the instability regions appear at higher frequency ratios for tensile loading as compared to corresponding compressive loading cases. The various other effects on the dynamic instability behaviour of the plate under tensile edge loading are

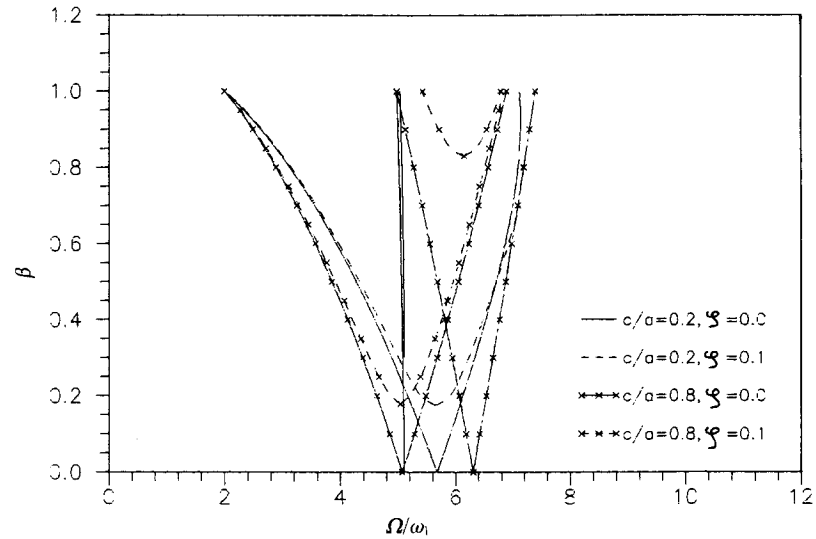

Fig. 8 Regions of dynamic instability for partial tensile edge loading at the centre (α=0.5. a/b=1).

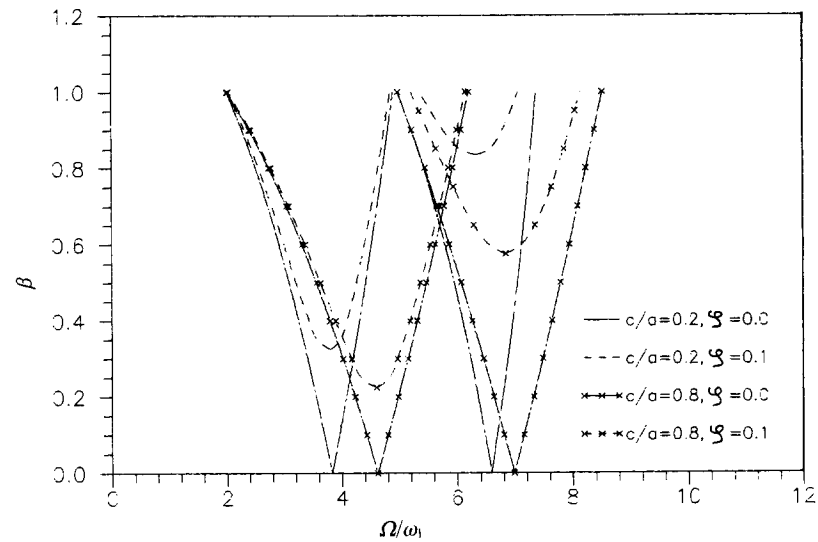

Fig. 9 Regions of dynamic instability for partial tensile edge loading at both ends (α=0.5. a/b=1).

as follows.

3.2.1. Effect of load band width and its position on the edge

For loading of small band width near the ends of the edges, the dynamic instability regions are usually smaller in width as can be observed from Fig. 6 and 9 for c/a=0.2 and from Fig. 7 for c/a=0.1. However, for the localized edge loading near the centre of the edges, the first instability region is usually wider in width while the width of the second instability region is small as can be observed from Fig. 7 for c/a=0.5 and Fig. 8 for c/a=0.2. This is because of

the fact that the second mode (mode 21) of dynamic instability is relatively insensitive to the static and dynamic load factors. Again, for nearly uniform edge loading, the widths of both instability regions are moderate as can be seen from Fig. 6 for $c/a=1.0$ and Fig. 8 and 9 for $c/a=0.8$.

3.2.2. Effect of static load factor

It has been observed that as the static load factor α increases, the parametric instability regions shift outwards on the frequency ratio axis and their widths decreases. These effects are just the opposite as were observed for the compressive loading cases.

3.2.3. Effect of damping

Effects of damping on the dynamic instability behaviour of the plate subjected to tensile edge loading can be observed from Figs. 6 to 9. The effects of damping, in general, are similar to those in the compressive loading cases. But in some cases, for higher values of dynamic load factor, it has been observed that the widths of dynamic instability regions become larger than those of corresponding undamped cases. This can be seen from Figs. 6, 7 and 8. This indicates rather destabilizing effects due to damping on instability regions as the dynamic loading parameter is increased.

The effects of damping on the dynamic instability behaviour of plates under different tensile edge loading cases are observed from Figs. 6 to 9. It can be seen that the damping has pronounced effects when the plate is subjected to localized tensile edge loading at one end or at both ends of the edges (Figs. 6, 7 and 9). As the width of the edge loading is increased, the critical dynamic load factor decreases (Figs. 6 and 9), indicating more susceptibility to instability. For concentrated edge loading, as the load moves from the end to the centre of the edges, the critical dynamic load factor corresponding to mode 11 of instability decreases while the second instability region corresponding to mode 21 does not exist for modal damping ratio of 0.1 and dynamic load factor as high as 1.0 (Fig. 8).

For partial edge loading at the centre of the edge, the damping has a moderate effect on the dynamic instability region corresponding to mode 11 as seen from Fig. 8. For mode 21, as the load band width is increased, the critical dynamic load factor decreases.

4. Conclusions

The results from a study of dynamic instability behaviour of a square plate subjected to localized compressive or tensile in-plane edge loading and the effects of damping on the dynamic instability behaviour can be summarized as follows.

(1) Dynamic instability results under compressive periodic edge loading show that the plate is less susceptible to instability under localized loading near the ends of the edge. The instability regions show larger effects for localized edge loading near the centre of the edge. For nearly uniform loading, the instability regions are moderate in effect.

(2) Dynamic instability results under tensile periodic edge loading show that the instability regions occur at higher frequency ratios as compared to the corresponding compressive loading cases. The effect of position of loading on the edge is similar to that of compressive loading case.

(3) The effect of damping on the instability regions shows that for both the compressive and tensile loading, there is a critical value of the dynamic load factor, beyond which the plate becomes dynamically unstable. The critical dynamic load factor increases as the damping increases. Damping generally reduces the widths of the instability regions.
(4) For both the compressive and tensile loading cases, the effects of damping are more pronounced for the localized loading near the ends of the edge as compared to those for localized loading near the centre or for uniform loading.

Notations

a, b	plate lengths in x- and y- directions respectively
c	load parameter
$[C]$	damping matrix
D	plate flexural rigidity
E	Young's modulus
h	plate thickness
k	shear correction factor
$[K]$	stiffness matrix
$[K_e]$	elastic stiffness matrix
$[M]$	mass matrix
P	edge load
P_{cr}	critical buckling load
$\{q\}$	nodal displacement vector
$[S]$	geometric stiffness matrix
t	time
w	deflection of mid-plane of the plate
x, y	cartesian co-ordinates
α, β	static and dynamic load factors respectively
γ	non-dimensional load
γ_{cr}	non-dimensional buckling load
λ	non-dimensional frequency
ν	Poisson's ratio
θ_x, θ_y	rotations of the normal about x- and y-axes respectively
ρ	mass density of the plate material
σ_x, σ_y, τ_{xy}	initial in-plane stresses
Ω	angular frequency of in-plane forcing function
ω	angular frequency of transverse vibration
ω_1	fundamental frequency of transverse vibration
ζ	modal damping ratio

Appendix

Finite element formulation of element matrices

1. Element elastic stiffness matrix:

$$[K_e]_e=\int_A [B]^T[D][B]dA$$

where A=element area,

$$[B]=[[B_1],\ [B_2],\ \cdots,\ [B_8]],$$

$$[B_i]=\begin{bmatrix} 0 & 0 & \dfrac{\partial N_i}{\partial x} \\ 0 & -\dfrac{\partial N_i}{\partial y} & 0 \\ 0 & -\dfrac{\partial N_i}{\partial x} & \dfrac{\partial N_i}{\partial y} \\ \dfrac{\partial N_i}{\partial x} & 0 & N_i \\ \dfrac{\partial N_i}{\partial y} & -N_i & 0 \end{bmatrix} \qquad i=1,\ 2,\ \cdots,\ 8,$$

N_i's are the shape functions corresponding to eight nodes,

$$[D]=\begin{bmatrix} D\begin{bmatrix} 1 & \nu & 0 \\ \nu & 1 & 0 \\ 0 & 0 & \dfrac{1-\nu}{2} \end{bmatrix} & [0] \\ [0] & \dfrac{kEh}{2(1+\nu)}\begin{bmatrix} 1 & 0 \\ 0 & 1 \end{bmatrix} \end{bmatrix}$$

2. Element geometric stiffness matrix:

$$[S]_e=\int_A [B_G]^T[\bar{\sigma}][B_G]dA$$

where $[B_G]=[[B_{G1}],\ [B_{G2}],\ \cdots,\ [B_{G8}]]$,

$$[B_{Gi}]^T=\begin{bmatrix} \dfrac{\partial N_i}{\partial x} & \dfrac{\partial N_i}{\partial y} & 0 & 0 & 0 & 0 \\ 0 & 0 & 0 & 0 & \dfrac{\partial N_i}{\partial x} & \dfrac{\partial N_i}{\partial y} \\ 0 & 0 & \dfrac{\partial N_i}{\partial x} & \dfrac{\partial N_i}{\partial y} & 0 & 0 \end{bmatrix} \qquad i=1,\ 2,\ \cdots,\ 8,$$

$$[\bar{\sigma}]=\begin{bmatrix} h[H] & & \\ & \dfrac{h^3}{12}[H] & \\ & & \dfrac{h^3}{12}[H] \end{bmatrix}$$

$$[H]=\begin{bmatrix} \sigma_x & \tau_{xy} \\ \tau_{xy} & \sigma_y \end{bmatrix}$$

3. Element mass matrix:

$$[M]_e=\int_A [N]^T[\bar{I}][N]dA$$

where $[N]=[[N_1],\ [N_2],\ \cdots,\ [N_8]]$,

$$[N_i]=\begin{bmatrix} N_i & & \\ & N_i & \\ & & N_i \end{bmatrix} \qquad i=1,\ 2,\ \cdots,\ 8,$$

$$[\bar{I}]=\begin{bmatrix} h & & \\ & \frac{h^3}{12} & \\ & & \frac{h^3}{12} \end{bmatrix}$$

The actual integration for element matrices are carried out by transformation of physical co-ordinates (x, y) into natural co-ordinates (r, s). Then the integrals are converted into forms convenient for numerical evaluation by Gauss-quadrature integration formula.

References

Bolotin, V. V. (1964), *The dynamic stability of elastic systems*, Holden-Day, San Francisco, U.S.A.

Caughey, T. K. and O'Kelly, M. E. J. (1965), "Classical normal modes in damped linear dynamic systems", *J. Appl. Mech., Trans. ASME*, **32**, 583-588.

Cederbaum, G. (1992), "Parametric excitation of viscoelastic plates", *Mech. of Str. and Mach.*, **20**, 37-51.

Chen, H. C. (1993), "Partial eigensolution of damped structural systems by Arnoldi's method", *Earthquake Engg. and Struct. Dynamics*, **22**, 63-74.

Engel, R. S. (1991), "Dynamic stability of an axially loaded beam on elastic foundation with damping", *J. Sound and Vibration*, **146**, 463-478.

Foss, K. A. (1958), "Coordinates which uncouple the equations of motion of damped linear dynamic systems", *J. Appl. Mech., Trans. ASME*, **25**, 361-364.

Hutt, J. M. and Salam, A. E. (1971), "Dynamic stability of plates by finite element method", *J. Eng. Mech. Div., ASCE*, **97**, 879-899.

Ioannides, E. and Grootenhuis, P. (1979), "A finite element analysis of the harmonic response of damped three-layer plates", *J. Sound and Vibration*, **67**, 2203-208.

Khan, M. Z. and Walker, A. C. (1972), "Buckling of plates subjected to localized edge loading", *The Structural Engineer*, **50**, 225-232.

Leissa, A. W. (1969), *Vibration of plates*, U.S. Govt. printing office, NASA SP-160., Reprinted in 1993 by the Acoustical Society of America.

Leissa, A. W. and Ayoub, E. F. (1988), "Vibration and buckling of a simply supported rectangular plate subjected to a pair of in-plane concentrated forces", *Journal of Sound and Vibration*, **127**, 155-171.

Leissa, A. W. and Ayoub, E. F. (1989), "Tension buckling of rectangular sheets due to concentrated forces", *J. Eng. Mech., ASCE*, **115**, 2749-2762.

Meirovitch, L. (1967), *Analytical methods in vibrations*, The McMillan Co., NY.

Rockey, K. C. and Bagchi, D. K. (1970), "Buckling of plate girder webs under partial edge loading", *Int. J. Mech. Sci.* **12**, 61.

Spencer, H. H. and Surjanhata, H. (1985), "Plate buckling under partial edge loading", *Developments in Mechanics (Proc. of the 19th Midwestern Mech. Conf.)*, **13**, 83-84.

Timoshenko, S. P. and Gere, J. M. (1961), *Theory of elastic stability (second edition)*, New York, McGraw Hill.